AMORPHOUS SILICON ALLOY PHOTOVOLTAIC TECHNOLOGY - FROM R&D TO PRODUCTION

S. GUHA,* J. YANG,* A. BANERJEE,* T. GLATFELTER,* K. HOFFMAN,*
S.R. OVSHINSKY,** M. IZU,** H. C. OVSHINSKY,** AND X. DENG**
*United Solar Systems Corp., 1100 West Maple Road, Troy, MI 48084
**Energy Conversion Devices, Inc., 1675 West Maple Road, Troy, MI 48084

ABSTRACT

The key requirements for photovoltaic modules to be accepted for large-scale terrestrial applications are (i) low material cost, (ii) high efficiency with good stability, (iii) low manufacturing cost with good yield and (iv) environmental safety. Thin films of amorphous silicon alloy are inexpensive; the products are also environmentally benign. The challenge has been to improve the stable efficiency of these modules and transfer the R&D results into production. Using a multijunction, multi-bandgap approach to capture the solar spectrum more efficiently, we have developed one-square-foot modules with initial efficiency of 11.8%. After 1000 h of one-sun light soaking, a stable efficiency of 10.2% was obtained. Both the efficiency values were confirmed by National Renewable Energy Laboratory. The technology has been transferred to production using an automated roll-to-roll process in which different layers of the cell structure are deposited in a continuous manner onto stainless steel rolls, 14" wide and half a mile long. The rolls are next processed into modules of different sizes. This inexpensive manufacturing process produces high efficiency modules with subcell yields greater than 99%. The key features of the technology transfer and future scope for improvement are discussed.

INTRODUCTION

There is a great need for a renewable, non-polluting energy source which can be used for generation of electricity for large-scale terrestrial applications. Photovoltaic (PV) modules are being used extensively for generation of electricity in remote areas; the cost, however, is still much higher than that produced by conventional fuels. In order for PV to be economically viable, the modules must have low material cost, they must show high efficiency with good stability and they must be easily manufacturable with good yield. Amorphous silicon (a-Si) alloys have attracted a great deal of attention [1] because only a thin layer (less than 1 μm) is needed to absorb the solar photons. The material cost of amorphous silicon PV panels is therefore low. The challenge has been how to improve stable efficiency and demonstrate manufacturability. In this paper, we describe our work to address these issues.

EFFICIENCY CONSIDERATIONS

Cell Efficiency

It is now well recognized that a multi-bandgap, multijunction approach offers the opportunity to obtain the highest stable efficiency for a-Si alloy solar cells [2]. A schematic

Mat. Res. Soc. Symp. Proc. Vol. 336. ©1994 Materials Research Society

diagram of a triple-junction structure is shown in Fig. 1. The top cell which captures the blue photons uses a-Si alloy with an optical gap of ~1.8 eV for the intrinsic (*i*) layer. The *i* layer for the middle cell is a-SiGe alloy with about 10% Ge. The optical gap is ~1.6 eV which is ideally suited for capturing the green photons. The bottom cell captures the red and the infrared photons and uses an *i* layer of a-SiGe alloy with about 40-50% Ge corresponding to an optical gap of ~1.4 eV. Light which is not absorbed in the cells gets reflected from the Ag/ZnO back reflector which is usually textured to scatter the light at an angle to facilitate multiple internal reflections.

The requirements to obtain high efficiency multijunction cells are the following: (1) high quality back reflector for efficient light trapping, (2) high efficiency component cells, (3) high quality doped layers to obtain good internal "tunnel" *p n* junctions with low electrical and optical losses and (4) optimum matching of the component cells.

The back reflector should perform two important functions. It must be highly reflecting; it should also scatter light at an angle higher than the critical angle for total internal reflection which, for a-Si alloy, is 16.6°. Ag is usually used to obtain high reflectivity. The interface between Ag and Si, however, is not highly reflecting because of intermixing of the two elements, and a buffer layer of ZnO is deposited in between to prevent intermixing. The required texture for optimum scattering is obtained by depositing Ag and ZnO at a high temperature in the range between 100 to 400 °C.

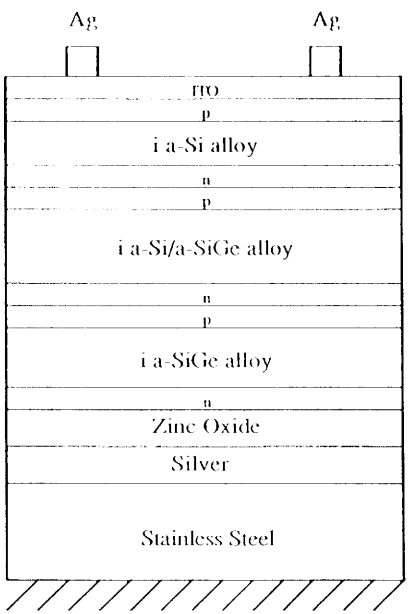

Fig. 1. Schematic diagram of a triple-junction cell structure.

The use of Ag/ZnO back reflector has resulted in significant gain [3,4] in short-circuit current density (J_{sc}) over specular stainless steel substrate. For a 4000 Å *i* layer of a-Si alloy, the gain is as much as 4 to 5 mA/cm^2. Theoretical calculations, however, show [5] that there is scope for much larger gain if there is total internal reflection without any loss at the reflecting surface. Experiments with different kinds of texture with different specular to diffusive reflection ratio show a remarkable insensitivity of J_{sc} to the degree of texture once a certain amount of texture is achieved [6]. It appears that there is a parasitic loss at the Si/ZnO and ZnO/Ag interface which limits J_{sc}. Elimination or reduction of this loss will have a large impact on cell efficiency, especially for the multijunction structure.

High efficiency component cells need high quality *i* layers. As mentioned earlier, we use a-Si alloy for the top cell and a-SiGe alloy for the middle and the bottom cells. In order to obtain high open-circuit voltage (V_{oc}) with good stability, we use hydrogen dilution of the gas mixture. Since the first [7] report of observation of improved stability with hydrogen dilution in a-Si alloy films, significant work has been carried out [8,9] to understand the role of excess hydrogen in the growth process. It is believed that hydrogen coverage of the growing surface gives the impinging species longer time to be incorporated and as a result gives a denser structure. For a-SiGe alloy we use [10] hydrogen diluted gas mixture of Si_2H_6 and GeH_4. We have shown earlier that since dissociation rates of Si_2H_6 and GeH_4 are similar, a gas mixture of Si_2H_6 and GeH_4 produces higher quality material than SiH_4 and GeH_4. Although significant advances have been made to improve the quality of a-SiGe alloy, the best quality a-SiGe alloy still has poorer transport properties than a-Si alloy. To achieve better collection from a given material, profiling of Ge-content in the cell has been used [11] to (a) provide increased built-in field and (b) generate the holes closer to the p-contact so that they do not have very far to move.

Typical initial performances for state-of-the-art component cells for the triple-junction structure are shown [12] in Table I. Also shown are the values after filtered one-sun (metal-arc lamp), 50 °C, 600 h light soaking. In this experiment, the component cells were degraded under open-circuit condition at 50 °C for 600 h and measured at 25 °C. The top cell was degraded under one sun and measured under AM1.5 illumination; the middle cell was degraded under one sun with a 530 nm cut-on filter and measured under AM1.5 illumination with the same filter; the bottom cell was degraded under one sun with a 630 nm cut-on filter and measured under AM1.5 illumination with the same filter. The top and middle cells were deposited on textured substrate without any back reflector, since in the multijunction configuration these cells do not see much reflected light. The bottom cells were deposited on our conventional Ag/ZnO textured back reflector. We notice a degradation of 10% to 20% after light soaking. We should mention that one can improve the initial performance by making the component cells thicker, but this results in larger degradation and lower light-degraded efficiency.

All the component cells in this study show true saturation in efficiency after prolonged light exposure. A typical example for the top and the bottom cell is shown in Fig. 2. The degradation is much lower than those obtained under intense light illumination, demonstrating the importance of thermal annealing of defects under normal operating conditions.

The doped layers play an important role in terms of providing high built-in potential in the bulk and also facilitating junctions between the adjacent cells without resistive loss. Since the doped layers are inactive as far as conversion of light to electricity is concerned, they must also be optically transparent. B-doping of a-Si alloy usually results in larger absorption in the material; the conductivity is also low resulting in large junction loss between the *p* and the *n* layers. We have developed [13] microcrystalline *p* layer with low optical loss. The layers are also highly conducting so as to provide high built-in potential and low tunnel junction loss [14].

Table I. Present status of typical initial and degraded cell parameters for component cells degraded and measured under conditions described in the text. The high- and the mid-bandgap cells use Cr as back reflector. Use of Ag/ZnO as back reflectors for these cells increases J_{sc} by 30% to 40%.

			J_{sc} (mA/cm^2)	V_{oc} (V)	FF	P_{max} (mW/cm^2)
a-Si	high-bandgap cell	initial	7.3	1.01	0.75	5.53
		degraded	7.2	0.98	0.71	5.01
		degradation (%)	1.4	3.0	5.3	9.4
a-SiGe	mid-bandgap cell	initial	7.02	0.77	0.65	3.51
		degraded	6.85	0.74	0.57	2.89
		degradation (%)	2.4	3.9	12.3	17.7
a-SiGe	low-bandgap cell	initial	7.8	0.67	0.64	3.34
		degraded	7.7	0.65	0.56	2.80
		degradation (%)	1.3	3.0	12.5	16.2

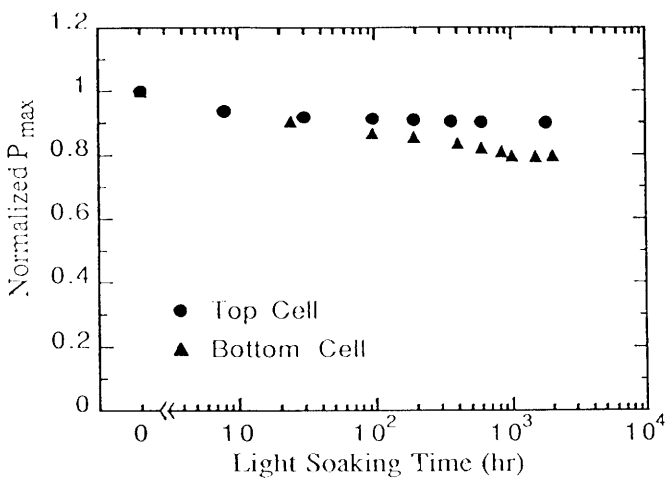

Fig. 2. Saturation in light-induced degradation of component cells.

For the fabrication of the multijunction cell, the next requirement is the matching of the component cells. The stability of the multijunction cell is primarily dictated by the performance of the component cell that limits the current. Since the top cell shows the maximum stability, it is desirable to design the structure top-cell limited, and small-area stable efficiency exceeding 11% has been achieved [15] using this approach.

Module Efficiency

In order to translate the small-area cell performance into modules, several key requirements need to be fulfilled. There has to be good uniformity over the deposited area; the optical loss due to encapsulation and current carrying grid-lines and the electrical loss due to transparent conducting oxide, grid-lines, etc. should be low. We use a monolithic approach in which the unit cell is a large-area cell of one-square-foot area. The grid design and the encapsulant are optimized to give an optical loss of ~2.1% and an electrical loss of ~2.4%. The total loss from average small-area efficiency to module is thus expected to be 4 to 5%.

A large number (about 200) of multijunction modules has been made over the last two years incorporating the optimizations outlined above. This resulted in a significant progress in the improvement of module efficiency as indicated in Fig. 3. The program on fabrication of one-square foot modules on Ag/ZnO back reflector started in September 1991, and in a period of about two years, the initial module efficiency has increased from 7.5% to 11.8%. The best results achieved to date are shown in Table II where the initial efficiencies for one-square-foot modules as measured at National Renewable Energy Laboratory (NREL) under a Spire 240A simulator are shown. Also shown are the measurements at NREL on modules from the same batch which have been light soaked under one-sun condition for 1000 h at 50 °C.

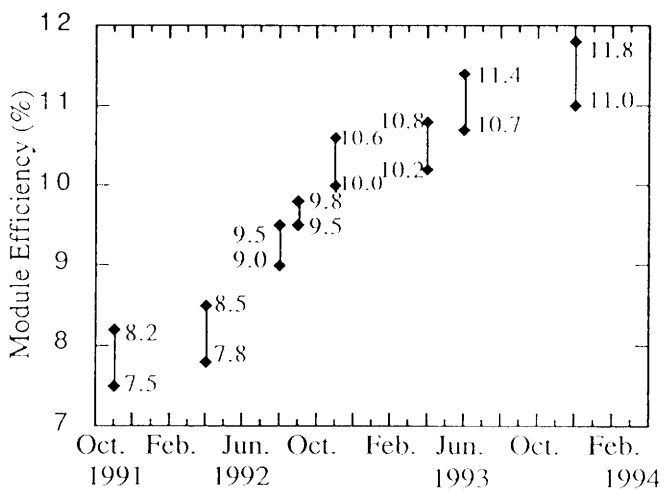

Fig. 3. Progress in initial module efficiency.

Table II. Summary of Module Results as Measured at NREL.

Sample	State	J_{sc} (mA/cm^2)	V_{oc} (V)	FF	η (%)
2452	Initial	7.25	2.400	0.675	11.75
2465	Initial	7.48	2.395	0.652	11.69
2437	Final	6.86	2.354	0.629	10.16
2445	Final	7.04	2.349	0.607	10.04
2447	Final	7.17	2.318	0.612	10.17

The stable module efficiency of 10.2% meets the important milestone of 10% stipulated for thin film PV modules to be acceptable for large-scale terrestrial applications. We should mention that as per NREL guidelines [16], the term "stable" refers to the performance level reached after 600 h of one-sun light soaking at 50 °C. As we have demonstrated earlier [17], our multijunction modules show saturation in degradation after about 600 h of one-sun light soaking at 50 °C. Because of thermal annealing effects, the degradation is lower at higher light soaking temperature and higher at lower temperature.

MANUFACTURING ISSUES

In order to translate the R&D results into production, the efficiency targets must be met with using a low-cost process with high yield. Energy Conversion Devices (ECD) pioneered a roll-to-roll method [18] of deposition of solar cells in which rolls of stainless steel, half-a-mile long, 14″ wide and 5 mil thick move in a continuous manner in four machines that serve the purpose of (i) washing, (ii) depositing the back reflector, (iii) depositing the a-Si alloy layers and (iv) depositing an antireflection coating. At United Solar, a fully automated roll-to-roll manufacturing line has been operational for many years [19] for depositing same bandgap double-junction cells. The coated web with the deposited cell is next processed to make a variety of lightweight, flexible and rugged products. The processing steps involve (i) cutting of the web into 16″ x 14″ slabs, (ii) scribing of ITO by screen printing, (iii) short and shunt passivation, (iv) screen printing of silver grid and (v) final assembly involving cell cutting and interconnection and lamination.

Typical stable module efficiency of the products is about 6% [20]. In order to improve the efficiency further, it is necessary to introduce many of the innovations described in the previous section into the manufacturing line. A triple-junction module manufacturing facility with an annual capacity of 2 MW has recently been designed and built [21] for Sovlux, a joint venture between ECD and Kvant, Moscow. The manufacturing line incorporated a Ag/ZnO back reflector sputtering machine to facilitate improved light trapping in the module. It also uses the triple-junction cell design in which the bottom cell uses a-SiGe alloy with bandgap profiling. The middle and the top cell use a-Si alloy deposited at different temperatures to change the bandgap.

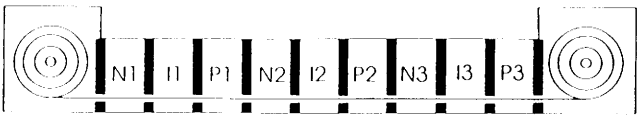

Fig. 4. Schematic diagram of roll-to-roll triple-junction a-Si alloy deposition machine.

The schematic diagram for the a-Si alloy deposition machine is shown in Fig. 4. The machine consists of a web payoff chamber, nine plasma-CVD chambers for the nine layers of the triple-junction cell and a take-up chamber. Stainless steel web, coated with Ag/ZnO, moves continuously through the chambers depositing the various layers sequentially. The process gas mixtures in each section are dynamically isolated from the adjacent chambers depositing the doped and undoped layers by proprietary "gas gates." The "gas gates" utilize laminar gas flow through constant geometrical cross-section conduits in a direction opposite to the diffusion gradient of the dopant gas concentration. SIMS analysis shows that one can eliminate migration of dopants to the undoped layer to a level below $10^{16}/cm^3$.

One of the key features in the a-Si alloy deposition machine is the provision for bandgap profiling of a-SiGe alloy in the bottom cell. This is achieved by using a proprietary gas distribution manifold and cathode configuration so that a gas mixture containing different amounts of GeH_4 is delivered into different parts of the chamber. The design was optimized to obtain any desired profile of Ge-concentration in the intrinsic layer.

For a PV production line, it is important to have appropriate evaluation of the cell performance such as cell efficiency, yield and uniformity through the entire production run. In our quality analysis (QA) process, statistical samples of 4″ x 14″ are selected from the production roll of 2500′ at an interval of 60′. Twenty-eight test solar cells of 7.35 cm^2 area (7 rows and 4 columns) are processed on each sample by the following procedures: (1) TCO scribing by screen printing of etching paste, heat curing and rinsing, (2) short and shunt passivation, and (3) screen printing of Ag paste grid.

The J-V data of 28 cells in a typical sample, sample 23 of run 109, is summarized in Table III. The efficiencies of all 28 cells are above 10%. The uniformity is excellent. The average V_{oc}, J_{sc}, FF and η are 2.37 V, 6.51 mA/cm^2, 0.673 and 10.41%, respectively, as shown in the table. With a subcell yield criterion of FF $\geq$ 0.55, the subcell yield of the sample is 100%. Figure 5 is a three-dimensional plot of subcell efficiency for every cell from the statistical QA/QC samples in a production run. Out of 1176 cells, only 3 show shunts or shorts. The results represent the excellent consistency, uniformity and yield achieved in a continuous roll-to-roll manufacturing process.

Table III. Performance Data of 28 Cells in a QA/QC Sample.

Cell No.	V_{oc} (V)	J_{sc} (mA/cm^2)	FF	Eff (%)	Cell No.	V_{oc} (V)	J_{sc} (mA/cm^2)	FF	Eff (%)
1	2.38	6.45	0.706	10.49	15	2.38	6.24	0.698	10.36
2	2.38	6.45	0.694	10.64	16	2.38	6.47	0.663	10.20
3	2.37	6.66	0.658	10.37	17	2.37	6.55	0.679	10.54
4	2.37	6.88	0.602	10.46	18	2.37	6.52	0.672	10.39
5	2.37	6.65	0.670	10.59	19	2.37	6.67	0.654	10.33
6	2.38	6.54	0.676	10.52	20	2.38	6.49	0.674	10.40
7	2.38	6.52	0.668	10.36	21	2.39	6.63	0.663	10.50
8	2.39	6.36	0.670	10.19	22	2.38	6.39	0.684	10.39
9	2.38	6.32	0.684	10.29	23	2.37	6.27	0.704	10.47
10	2.37	6.35	0.686	10.30	24	2.37	6.43	0.695	10.59
11	2.37	6.88	0.633	10.31	25	2.37	6.53	0.679	10.50
12	2.37	6.52	0.671	10.36	26	2.37	6.66	0.652	10.30
13	2.38	6.39	0.688	10.45	27	2.38	6.67	0.651	10.34
14	2.39	6.71	0.669	10.72	28	2.38	6.37	0.674	10.21
					Average	2.37	6.51	0.673	10.41

Yield for cells with FF ≥ 0.55: 100%

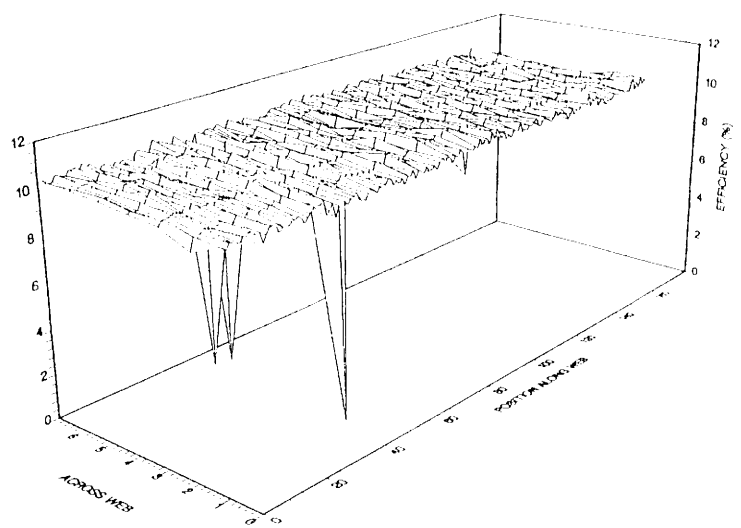

Fig. 5. Three dimensional plot of cell efficiency of test cells in a production run.

Table IV. Initial Module Performance Data of Four-square-foot Modules Produced in the Manufacturing Line.

Module	V_{oc} (V)	I_{sc} (A)	FF	η	Measurement Lab
23	21.62	2.68	0.628	9.31	ECD
	21.56	2.72	0.63	9.46	NREL
27	21.6	2.72	0.632	9.48	ECD
28	21.3	2.75	0.634	9.47	ECD
30	21.61	2.68	0.63	9.36	ECD
	21.51	2.74	0.627	9.47	NREL

Modules of four-square-foot area (1′ x 4′) were fabricated by interconnecting 9 strip cells for obtaining approximately 16 V at maximum power point. Typical results are shown in Table IV. Note that initial aperture area efficiencies in the range of 9.4 to 9.5% have been confirmed both at ECD and NREL. The modules were light soaked under one sun for 2000 h at a temperature between 50 to 60 °C. The degradation behavior is shown in Fig. 6. We note that the stabilized efficiency is 8%.

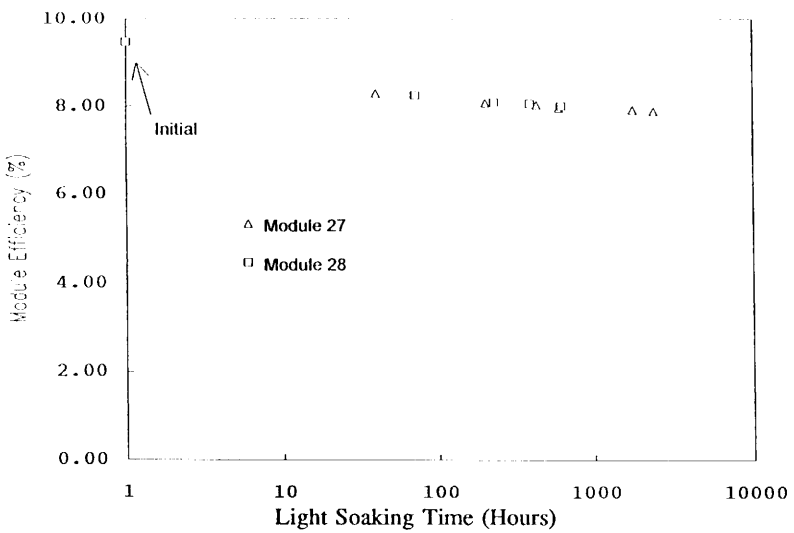

Fig. 6. Module efficiencies of two 4 ft^2 modules as a function of light soaking time under one-sun illumination.

The manufacturing line is still being optimized, and it is important to discuss how the gap between 10% stabilized efficiency in R&D and 8% from the manufacturing line can be bridged. The middle cell in the latter case does not contain any germanium. This limits the short-circuit current from the cell and lowers the efficiency. The deposition rate of the top cell is high (> 10 Å/s). Use of somewhat lower deposition rate and higher hydrogen dilution as discussed earlier will improve the module efficiency further.

FUTURE DIRECTIONS

Although the achievement of 10% stable module efficiency addresses the important issue of near-term market acceptability, the multijunction approach holds promise for much higher efficiency. The component cell requirement for 15% module efficiency has been addressed by Guha et al. [17]. Typical characteristics necessary vis-a-vis the current status at United Solar are shown in Table V. Improvement in material quality, especially for the low bandgap alloy, will be necessary to meet that goal. Use of novel plasma deposition methods [22] in which the growth kinetics can be controlled by selecting suitable species to impinge on the growing surface will play a key role in improving the stable material quality. Further investigation of the role of microstructure, hydrogen bonding and impurities on stable device performance for materials deposited under different conditions will help us to have a better understanding of the issues involved. Reduction of losses in the back reflector will also improve the efficiency. With a well-focussed sustained approach encompassing both material and device research, the progress in improvement of stable module efficiency can surely be maintained.

Table V. Component cell stabilized parameters for 15% module efficiency. (Present status at United Solar shown in parentheses.)

	Voc (V)	FF	J_{sc} (mA/cm^2)	Power (mW/cm^2)
Top Cell$^+$	1.1 (0.98)	0.75 (0.71)	8.2 (7.7)	6.8 (5.3)
Middle Cell^{*+}	0.89 (0.74)	0.70 (0.57)	8.4 (6.9)	5.2 (2.9)
Bottom Cell$^{\Delta}$	0.68 (0.65)	0.68 (0.56)	8.6 (7.7)	4.0 (2.8)
Devices	2.67	0.72	8.3	16.0

$^+$ Without back reflector
* Under λ>530 nm light
$^{\Delta}$ Under λ>630 nm light

CONCLUSIONS

General considerations for obtaining high stabilized solar cell and module efficiencies using a-Si alloy are discussed. Using a multi-bandgap, multijunction approach, a stable efficiency of 10.2% has been achieved on a one-square-foot panel. A manufacturing line has been designed and built to translate the R&D results into a low-cost production process with high yield. Further scope for improvement in efficiency is discussed.

ACKNOWLEDGEMENT

The authors would like to thank X. Xu, A. Krisko and K.L. Narasimhan for discussions and collaboration, V. Trudeau for preparation of the manuscript, and National Renewable Energy Laboratory for supporting the program under Subcontract Nos. ZM-1-19033-2 at United Solar Systems Corp. and ZM-2-1104-7 at Energy Conversion Devices, Inc.

REFERENCES

1. See, for example, Mat. Res. Soc. Symp. Proc. **297** (1993).
2. S. Guha, Mat. Res. Soc. Symp. Proc. **149**, 405 (1980).
3. A. Banerjee and S. Guha, J. Appl. Phys. **69**, 1030 (1991).
4. A. Banerjee, J. Yang, and S. Guha (to be published).
5. E. Yablonovitch and G. Cody, IEEE ED-**29**, 300 (1982).
6. S. Guha, Optoelectronics **5** (2), 201-207 (1990).
7. S. Guha, K.L. Narasimhan, and S.M. Pietruszko, J. Appl. Phys. **52**, 859 (1981).
8. K. Tanaka and A. Matsuda, Mat. Sci. Reports **2**, 139 (1987).
9. A. Gallagher, SERI Technical Report, SERI/TP-211-3747 (1990).
10. S. Guha, J.S. Payson, S.C. Agarwal, and S.R. Ovshinsky, J. Non-cryst. Solids **97-98**, 1455 (1987).
11. S. Guha, J. Yang, A. Pawlikiewicz, T. Glatfelter, R. Ross, and S.R. Ovshinsky, Appl. Phys. Lett. **54**, 2330 (1989).
12. X. Xu, J. Yang, and S. Guha, Proc. 23rd IEEE PVSC, Louisville, KY, 971 (1993).
13. S. Guha, J. Yang, P. Nath, and M. Hack, Appl. Phys. Lett. **49**, 218 (1986).
14. A. Banerjee, J. Yang, T. Glatfelter, K. Hoffman, and S. Guha, Appl. Phys. Lett. **64**, 1517 (1994).
15. J. Yang and S. Guha, Appl. Phys. Lett. **61**, 2917 (1992).
16. W. Luft, B. Stafford, and B. von Roedern, in Amorphous Silicon Materials and Solar Cells, AIP Conf. Proc. No. 234, edited by B. Stafford (American Institute of Physics, New York, 1991), p. 3.
17. S. Guha, J. Yang, A. Banerjee, T. Glatfelter, K. Hoffman, and X. Xu, PVSEC-7, 43 (1993).
18. M. Izu and S.R. Ovshinsky, SPIE Proc. **407**, 43 (1983).
19. P. Nath, K. Hoffman, J. Call, C. Vogeli, M. Izu, and S.R. Ovshinsky, PVSEC-3, 395 (1987).
20. W. Luft, B. von Roedern, B. Stafford, D. Waddington, and L. Mrig, Proc. 22nd IEEE PVSC, Las Vegas, NV, 1393 (1981).
21. M. Izu, X. Deng, A. Krisko, K.Whelan, R. Young, H.C. Ovshinsky, K.L. Narasimhan, and S.R. Ovshinsky, Proc. 23rd IEEE PVSC, Louisville, KY, 919 (1993).
22. S.R. Ovshinsky, Solar Energy Materials (in press).

This article appears in Mat. Res. Soc. Symp. Proc. Vol. 345